

Raman scattering and electrical characterization of AlGaAs/GaAs rectangular and triangular barriers grown by MOCVD

J. Díaz-Reyes*

CIBA-IPN

Ex-Hacienda de San Juan Molino Km. 1.5,
Tepetitla, Tlaxcala. 90700. México

M. Galván-Arellano and R. Peña-Sierra

CINVESTAV-IPN, Depto. de Ing. Eléctrica, SEES

Apdo. Postal 14-740, México, D. F. 07000. México

(Recibido: 20 de octubre de 2009; Aceptado: 20 de enero de 2010)

It presents the structural and electrical characterization of rectangular and triangular barriers based on $\text{Al}_x\text{Ga}_{1-x}\text{As}/\text{GaAs}$ heterostructures grown in a metallic-arsenic-based-MOCVD system. The gallium and aluminum precursors were the organometallic compounds trimethylgallium and trimethylaluminum, respectively. The barriers were grown with different aluminum concentrations for varying the AlGaAs bandgap and as consequence the potential barrier height. To obtain the triangular barriers increased the Al concentration gradually each minute up to reach 40% molar fraction. Raman spectroscopy was used to the structural characterization of the barriers. Potential barrier height and carrier transport mechanism through them is obtained by the current-voltage measurements. Raman spectra of the rectangular barrier present the TO GaAs-like, LO GaAs-like and LO AlAs-like as main vibrational modes. As the growth temperature is increased the layers compensation decreases but the Raman spectra show that the layers become more defective. The triangular barriers Raman spectra presented the same vibrational modes. As the Al concentration is increased the Triangular barriers phononic bands shifted slightly to lower wavenumbers and are broader compared with the phononic bands of the rectangular barriers.

Keywords: Semiconductors III-V; GaAs; Barrier height; Raman spectroscopy; MOCVD

1. Introduction

Ternary AlGaAs epitaxial layer grown on GaAs substrate is the most promising material for the fabrication of visible light emitting diodes (LED), laser diodes (LD) and solar cell application [1, 2]. High brightness visible LED at 655 nm was fabricated by AlGaAs DH structure on lattice matched GaAs substrate [2]. MOCVD is a simple and suitable technique for the preparation of high quality epitaxial layer using group III metallic. High brightness visible LED at 655 nm was fabricated by AlGaAs DH structure on lattice matched GaAs substrate. Graded composition at the AlGaAs/GaAs interface has increased the short circuit current and reduced surface recombination velocity.

The high control grade that has on the doping, thickness control and composition of these and other more complex semiconductor, with the most modern techniques for epitaxial deposit by MBE and MOCVD, has given a notable impulse to design and construction of new devices or well to the optimization of the ones already known as the semiconductor laser diodes with quantum well (QW). Among the new devices that incorporate AlGaAs/GaAs heterostructures can mention the frequency conversion mixers [3], graded barrier photodetectors [4], etc. These devices base their operation in a unipolar barrier of constant or graded composition. Even and when there is a lot of applications no has given enough importance to the study of the conduction mechanisms at that barrier type, which is one the objectives of this work: the determination

of the conduction mechanisms in barriers based in AlGaAs and GaAs.

Raman scattering is a versatile non-destructive tool for characterization of semiconductor heterostructures and devices like laser, short wave communication photodetector, HEMT, etc. [5]. Raman scattering strongly depends on lattice excitation and LO phonons which couple strongly with collective oscillation of plasmons because of the macroscopic electric fields associated with excitations in back scattering geometry [5].

Figure 1 illustrates the basic structure to study. The barrier height is formed by the inclusion of AlGaAs, by varying the alloy composition from 0 up to 0.4 mol. A bandgap of about 2.15 eV is obtained and the barrier extension has a constant length of 0.58 μm . The conduction mechanisms that could be present in unipolar barriers depend of three main factors: the barrier height that generates in the heterostructure (Φ_B) compared with the thermal voltage value, barrier extension compared with the media free trajectory of electrons and the presence of recombination centers in AlGaAs layer.

The main electrical transport mechanisms present in the barriers are tunnelling, thermionic emission and electrical transport limited by recombination centers in the barrier region, this latter one is known as Poole-Frenkel. Our case the barriers extension is 0.58 μm . Thus, the carrier transport by tunnel effect is neglected. So, the predominant mechanisms in the structures may be thermionic emission and Poole-Frenkel.

*e-mail: jdiazr2001@yahoo.com

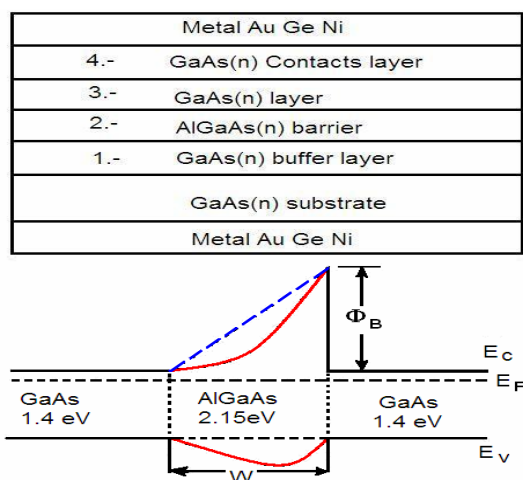


Figure 1. Scheme and band-gap diagram of the used heterostructure. The dashed line represents ideal band gap for the triangular barriers.

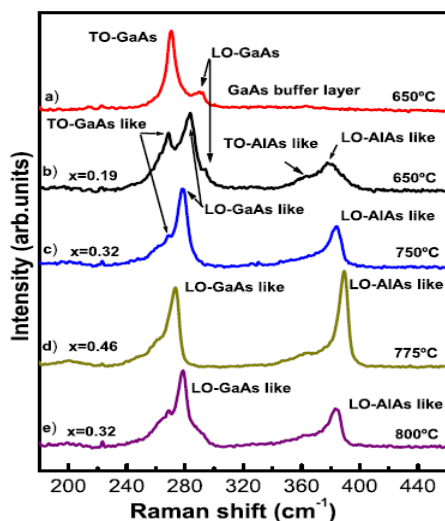


Figure 2. Raman scattered spectra of $\text{Al}_x\text{Ga}_{1-x}\text{As}/\text{GaAs}$ rectangular barriers grown at different substrate temperatures by MOCVD.

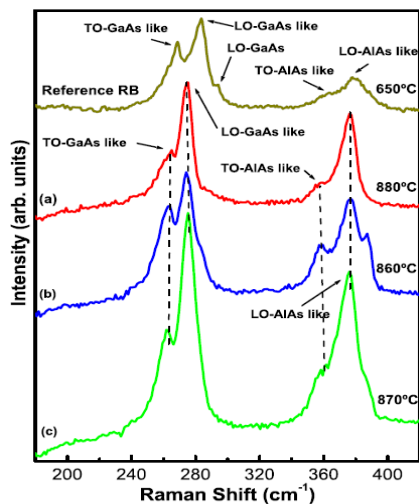


Figure 3. Raman spectra of $\text{Al}_x\text{Ga}_{1-x}\text{As}/\text{GaAs}$ triangular barriers.

2. Experimental details

The $\text{GaAs}/\text{Al}_x\text{Ga}_{1-x}\text{As}/\text{GaAs}$ heterostructures were grown in a metallic-arsenic-based-MOCVD reactor at horizontal configuration of two zones and hot walls. The samples are grown on (100) GaAs substrates. The main characteristics and the details of the growth conditions have been published elsewhere [6]. The precursors of gallium and aluminum were trimethylgallium (TMG) and trimethylaluminum (TMAI), metallic arsenic of 7N was used as arsenic source. The heterostructures are constituted by four layers grown on n-type GaAs substrate with a carrier concentration of 10^{18} cm^{-3} . The four layers are the following: a GaAs buffer layer, an AlGaAs layer that forms the potential barrier, the third one is a GaAs layer and the last one is a GaAs layer that is highly doped with silicon with a concentration about 10^{18} cm^{-3} . The electron concentration in the AlGaAs layer is controlled by the aluminum molar fraction of the alloy and by the growth temperature. It explored the growth temperature range of 650 to 800°C.

The objective of the first layer is to impede the diffusion of substrate crystalline defects toward the structure. This GaAs layer is grown making to flow TMG on the sample surface during a growth time of 30 min for obtaining a thickness of $0.45 \mu\text{m}$, in accordance with previous studies the electron concentration could be about 10^{17} cm^{-3} [6]. The second layer is of $\text{Al}_x\text{Ga}_{1-x}\text{As}$; at this point the barrier height and width can be determined, with a growth time of 14 min results a thickness of $0.58 \mu\text{m}$. This layer is grown by making to flow TMG and As, as for the latter layer, and the TMAI for rectangular barrier kept constant and for triangular barrier varied from 0 up to 34% with increments of 2% per minute. The AlGaAs results to be highly resistivity when the growth temperature is around 700°C; in the experimental conditions that was grown this layer has a resistivity higher at $10 \Omega\text{cm}$, that increases to increase the aluminum molar fraction in alloy. The third layer is similar at the first one and has a thickness of $0.13 \mu\text{m}$.

In order to have better ohmic contacts, after the third layers a fourth GaAs layer highly doped with Si with a concentration of 10^{18} cm^{-3} . The electrical characterization of potential barriers was carried out by I-V-T measurements in a Keythley and a Lake Shore cryostat with temperature controller (model 330) that allows to vary the temperature in the range of -200 to 120°C. The diagram of the used heterostructure is presented in Fig. 1, as well as the band gap diagram. The investigated samples were square shaped with dimensions of $5.0 \times 5.0 \text{ mm}^2$ and thickness of $0.48\text{--}2.97 \mu\text{m}$. The samples were provided with four ohmic contacts by alloying indium small balls on the corners of the samples, for alloying the contacts to surface sample, these were annealed at a temperature of 400°C for 1 min in an atmosphere of nitrogen. The linearity and symmetry of the ohmic contacts were tested following the procedure described in the ASTM standards [7].

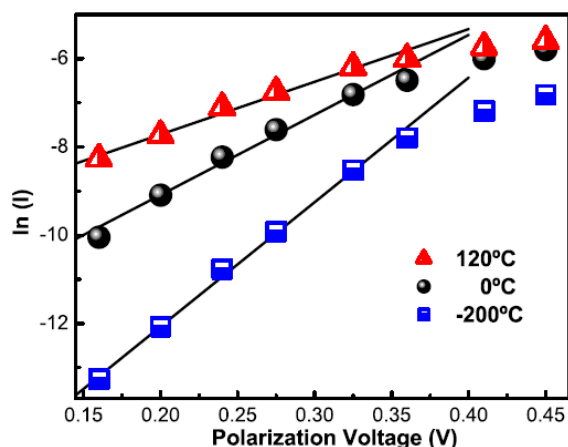


Figure 4. Plot of $\ln(I)$ vs. V for an AlGaAs/GaAs barrier at three different temperatures.

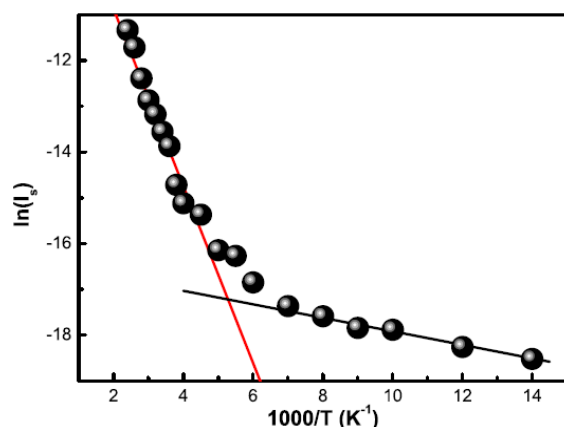


Figure 5. Plot of $\ln(I_s)$ vs. $1/T$ for an AlGaAs/GaAs sample.

Table 1. Barriers height for typical heterostructures

Sample	Φ_B (eV)
rectangular	0.189
triangular	0.438
triangular	0.560

Raman scattering experiments were performed at room temperature using the 6328 Å line of a He-Ne laser at normal incidence for excitation. The laser light was focused to a diameter of 6.0 μm at the sample using a 50x (numerical aperture 0.9) microscope objective. The nominal laser power used in these measurements was 20 mW. Scattered light was analyzed using a micro-Raman system (LabRam model of Dilor), a holographic notch filter made by Kaiser Optical System, Inc. (model superNotch-Plus), a 256x1024-pixel CCD used as detector cooled to 140 K using liquid nitrogen, and two interchangeable gratings (600 and 1800 g/mm). Typical spectrum acquisition time was limited to 60 s to minimize the sample heating effects. Absolute spectral feature position calibration to better than 0.5 cm^{-1} was performed

using the observed position of Si which is shifted by 521.2 cm^{-1} from the excitation line.

The main goal of the work is to study the electrical transport mechanism in the barriers as rectangular and triangular. Besides, we studied the structural quality of the different heterostructures.

3. Results and discussion

The morphological characteristics of the $\text{Al}_x\text{Ga}_{1-x}\text{As}$ epitaxial layer are very sensible to the growth temperature. At low temperatures mirror like surfaces were obtained, as the growth temperatures (T_G) reached about 750°C microscopic features appeared on the surfaces. Those morphological features are oval defects and some other kind of typical MOCVD defects as those due to the beginning of the homogeneous phase growth regime as the substrate temperature is increased. For temperatures greater than 800°C the surface appeared hazy and in some cases eventually becomes polycrystalline as was examined by X-ray measurements.

Figure 2 shows Raman scattering results of rectangular $\text{Al}_x\text{Ga}_{1-x}\text{As}$ heterostructures grown by MOCVD at several growth temperatures (T_G) using metallic arsenic as arsenic precursor. As back scattering geometry has been used to record the Raman spectra of GaAs (100) substrate as is shown in Fig. 2. As the transverse optical phonon (TO) frequency is forbidden in this scattering geometry and only the longitudinal phonons (LO) should appear. In figure the Raman spectrum for a GaAs epilayer (spectrum (a)) is included as reference; the corresponding layer was grown with the same experimental conditions that those ones used for the GaAs buffer layer. In spectrum (a) the TO and LO GaAs modes located at 268 and 292 cm^{-1} , respectively, are clearly distinguishable. In the Raman spectrum (b), the peaks sited at 283.4, 363.2 and 378.7 cm^{-1} are assigned to the modes LO-GaAs like, TO-AlAs like and LO-AlAs like, respectively, and they are originated from the ternary alloy. Due to the thickness of the $\text{Al}_x\text{Ga}_{1-x}\text{As}$ epilayers, the modes corresponding to GaAs could not be assigned to the buffer layer. A possible explanation of the presence of the GaAs-like TO phonon and AlAs TO phonon is the probable existence of crystalline defects in the epitaxial layers. The small shoulder on the low-frequency side of the GaAs-like LO phonon is the GaAs-like TO mode, in principle forbidden in the experimental geometry. Its appearance indicates that the crystal quality of the AlGaAs layers is not perfect, but its small intensity indicates that the quality is good. The forbidden modes are more clearly observed in samples grown with the extreme growth conditions. It suggests that the crystal quality of the AlGaAs epilayers degrades either when the growth temperature was lower than 650°C or was increased above 800°C. The GaAs-like LO phonon peak shifts lightly toward the lower energy side and AlAs like LO phonon on the higher energy side and this feature is due to the reduction of mismatch at the interface because of the composition grading from surface to interface. The Al composition of the $\text{Al}_x\text{Ga}_{1-x}\text{As}$ layer

can be determined using the fitted curves that relate the LO-phonon frequency with the aluminum content in the $\text{Al}_x\text{Ga}_{1-x}\text{As}$ system, according to the next equations [6]:

$$\omega_{LO}^{GaAs}(x) = 290.2 - 36.7x \text{ cm}^{-1} \quad (1)$$

$$\omega_{LO}^{AlAs}(x) = 364.7 + 46.7x - 9.4x^2 \text{ cm}^{-1} \quad (2)$$

The Al molar fraction of the ternary films can be found from the spectrum (b), and in accordance with the LO-GaAs like and LO-AlAs like peak positions, this is $x \sim 0.19$. As mentioned earlier, in the spectrum corresponding to the GaAs epilayer, only the LO and TO modes for GaAs are visible. For the spectra corresponding to the samples grown at $T_G = 750, 775$ and 800°C (c, d, and e, respectively), the LO-GaAs like and TO-GaAs like modes appear as small contributions of the main band. The calculated Al compositions for these samples were: $x \sim 0.32$ for $T_G = 750^\circ\text{C}$, $x \sim 0.46$ for $T_G = 775^\circ\text{C}$ and $x \sim 0.32$ for $T_G = 800^\circ\text{C}$. Thus, a homogeneous behavior of the Raman signals of the $\text{Al}_x\text{Ga}_{1-x}\text{As}$ films for growth temperatures above to 750°C is observed, whereas for growth temperatures below 750°C the signals arising from the buffer GaAs layer present an important contribution to the total spectrum. It suggests that the crystalline quality of the AlGaAs epilayers was degraded either when the growth temperature was lower than 650°C or higher than 800°C for the rectangular barrier.

Figure 3 illustrates Raman scattering results of $\text{Al}_x\text{Ga}_{1-x}\text{As}$ triangular barriers grown at three different substrate temperatures and in each one is increased the aluminum in gradual form for obtaining the triangular barrier. In Fig. 3 the Raman spectrum (a) for AlGaAs barrier with constant aluminum composition is included for comparing the behavior of the Raman spectra of triangular barriers. As can be observed the Raman spectra of the triangular barriers present the same main features than the previous ones but the peaks are slightly displaced toward high-frequencies as the aluminum is increased, this is opposed the case of triangular barriers [8]. The GaAs-like and AlAs-like phonon peaks shift toward the higher energy side and these features are due to the reduction of mismatch at the interface because of the composition grading from surface to interface, this fact is indicated in Fig. 3 by dashed lines. In spectrum (b), the signals at 265, 275, 368 and 376 cm^{-1} are assigned to the modes TO-GaAs like, LO-GaAs like, TO-AlAs and LO-AlAs like in comparison with the reference RB. These are originated on the graded ternary alloy as already mentioned above [6]. Increase of aluminum in layers becomes evident only in the broader of the vibrational modes bands. The LO-GaAs like is enhanced as the aluminum concentration is increased becoming the dominant signal followed for the LO-AlAs like. These results indicate that the heterostructures are of good crystalline quality which can be used for optoelectronic devices with triangular barriers. The line width of the main LO modes increases with

increase in the Al gradual composition and also become more intense, as can see in Fig. 3.

Figure 4 illustrates the results of the current-voltage (I-V) measurements for a typical rectangular sample, where one can be observed clearly the rectification effect. To analyze the electric behavior of the structures measurements I-V for different samples and several temperatures were performed. By linear fit at small polarization voltages, the straight line interception at $V=0$ provides the saturation current (I_s) of the structure. As observed in figure, the straight line slope changes as function of the temperature and besides as the polarization voltage is increased. A strong variation of the current with temperature is observed. This behavior could suggest that thermionic emission current is the dominant conduction mechanism. However, it requires a deeper analysis due to that the fit could not make for whole the polarization voltage range, of here that maybe present other conduction mechanisms.

At one first approximation may consider valid data for the saturation current estimated above. Fig. 5 illustrates the plot $\ln(I_s)$ vs T^{-1} , in which one observes clearly two slopes which should suggest that are present at least two conduction mechanisms clearly dependent of the temperature. In order to determinate weather effectively there is thermionic emission, a study of $\ln(I/T^2)$ as function of $1/T$ taking the polarization voltage as parameter using the following equation is done.

$$I/T^2 = A^* \exp \left[-\frac{q}{k_B T} (\Phi_B - V) \right] \quad (3)$$

In this way one can obtain an activation energy whose meaning will depend on the mechanism than greater influence has in the conduction process. If the electron transport on the barrier is a thermionic process, then the barrier height may be obtained directly from the fit to the equation, where A^* is the Richardson's constant. For the ternary compound, $\text{Al}_{0.3}\text{Ga}_{0.7}\text{As}$, the value of A^* is $11.2288 \text{ A/cm}^2\text{K}^2$. This equation allows to obtain the value of Φ_B for the three studied samples, which are presented in table 1 [9]

Although, the values are consistent with the barriers height calculated by the difference of band-gap between GaAs and AlGaAs, one can observe that the slope of the current behavior changes as function of the temperature and the applied polarization voltage.

The current behavior of heterojunctions can be described very well when the polarization voltage is smaller than 0.5V and the temperature is higher than 250 K , this could indicate that the conduction mechanism is the thermionic emission. At low temperatures there are not significant changes, even between different samples, the tendency is very similar in all ones. Due to current changes notably with temperature, more than tunnel current through the barrier, it may suggest that the mechanism involves be Poole-Frenkel emission.

One of the properties of these heterostructures is the small capacitance and the small variations with the applied voltages. The results for the triangular barriers indicate that the capacitance is practically the same in wide polarization range. In the polarization range, from -8 volts to 2 volts, the capacitance passed only of 9.1×10^{-11} up to 9.4×10^{-11} farads [9].

4. Conclusions

We have grown heterojunctions for forming rectangular and triangular barriers, based in the AlGaAs/GaAs system. In the growth system used for making them one can give them predetermined form, can decide their height and extension. By Raman scattering was found that the crystalline quality is good because of the small shoulder on the low frequency of the LO GaAs-like phonon is the TO GaAs mode, forbidden in principle in the experimental geometry, and it can be assigned to the high residual impurity of the AlGaAs layers.

The I-V measurements indicate that by the extension of the triangular barrier, the mechanism predominant is thermionic emission over the barrier when the temperature is high and the polarization voltages are small. At low temperatures (<200 K) the influence of the ionization of recombination centers by influence of the electric field was observed.

The measured capacitance is small and barely changes with the polarization voltages; this characteristic is one of the advantages than have these structures for the p-n junctions or Schottky barriers.

References

- [1] J. S. Shea, B. T. You, J. Y. Kao, Y. R. Deng, J.S. Chang, T. P. Chen. *J. Cryst. Growth* **128**, 533 (1993).
- [2] B. T. You, J. S. Shea, J. Y. Kao, Y. R. Deng, Y. S. Chang, C.Y. Juan, T.P Chen. *J. Cryst. Growth* **128**, 527 (1993).
- [3] T.L. Tansley, S. Giugni, M.J. Batty, G.J. Griffiths. *Thin Solid Films*, **163**, 479 (1988).
- [4] C. Y. Chen, A. Y. Cho, P. A. Garbinski, C. G. Bethea and B. F. Levine. *Appl. Phys. Lett.* **39**, 340 (1981).
- [5] P. Parayanthal, F. H. Pollak. *Phys. Rev. Lett.* **52**, 1822 (1984).
- [6] J. Díaz-Reyes, R. Castillo-Ojeda, M. Galván-Arellano and R. Peña-Sierra. *Superficie y Vacío* **15**, 22 (2002).
- [7] ASTM Standard test Methods for Measuring Resistivity and Hall Coefficient and Determining Hall Mobility a Single-Crystal Semiconductors. ASTM, F76-86, Oct.31, 1986.
- [8] K. Jeganathan, V. Ramakrishnan and J. Kumar. *Cryst. Res. Technol.* **34**, 1293 (1999).
- [9] A. Méndez-Fernández, "Estudio y caracterización de defectos profundos en GaAlAs obtenidos por MOCVD". Master Science Thesis. CINVESTAV-IPN. December 1995.